Structure and Properties of the Transition-Metal Zintl Compounds $A_{14}MnPn_{11}$ (A = Ca, Sr, Ba; Pn = As, Sb)

Anette Rehr,[†] Traci Y. Kuromoto,[†] Susan M. Kauzlarich,*[,†] J. Del Castillo,[‡] and David J. Webb*[,‡]

Departments of Chemistry and Physics, University of California, Davis, California 95616

Received August 25, 1993. Revised Manuscript Received November 1, 1993[⊗]

The compounds $A_{14}MnPn_{11}$ (A = Ca, Sr, Ba; Pn = As, Sb), have been synthesized by reacting the elements in stoichiometric amounts in welded Nb tubes sealed in quartz ampules at high temperature (1250 °C). Single-crystal X-ray data (130 K, tetragonal, $I4_1/acd$ (142), $Z = 8$) were refined for all compounds except $Ba_{14}MnAs_{11}$: $a = 16.688$ (8) Å, $c = 22.266$ (9) Å ($R = 5.82\%$, $R_w = 6.95\%$, $Ca_{14}MnSb_{11}$); $a = 17.511$ (4), $c = 23.321$ (7) Å, ($R = 4.07\%$, $R_w = 3.93\%$, $Sr_{14}MnSb_{11}$); $a = 18.394$ (3), $c = 24.069$ (6) Å ($R = 7.52\%$, $R_w = 6.96\%$, $Ba_{14}MnSb_{11}$); $a = 15.754$ (3), $c = 21.037$ (7) Å ($R = 4.09\%$, $R2 = 8.82\%$, $Ca_{14}Mn\ As_{11}$); $a = 16.576$ (10), $c = 22.167$ (14) Å ($R = 5.70\%$, $R_w = 4.87\%$, $Sr_{14}MnAs_{11}$). These compounds are isostructural to the main-group Zintl compound $Ca_{14}AlSb_{11}$. Magnetization measurements performed on powder samples have shown that the antimony compounds are ferromagnets with ordering temperatures of 65 (Ca), 45 (Sr), and 20 K (Ba), whereas the arsenic compounds are paramagnetic down to 5 K. The temperature dependence of the resistivity of pressed pellets indicates that the Sb compounds may be metallic and the As compounds are semiconductors.

Introduction

Zintl phases form a large family of compounds whose electronic structures conform to the $8-N$ rule or the Zintl–Klemm concept.[1] The initial phases which Zintl discussed were binary compounds composed of an alkali or alkaline earth metal, A, and a heavier main-group element, X. Zintl proposed that the structures and properties of these compounds could be understood by simple chemical bonding considerations. The electropositive alkali or alkaline earth metal, A, donates its electrons to the electronegative element, X, which forms the necessary number of homoatomic bonds so that each element has a complete octet.[2] This simple formulism has been expanded to include ternary compounds so that now the anionic structure can be derived from homo- and heteroatomic bonds.[3,4] Zintl compounds are electronically located between insulators and intermetallic phases. Borderline cases of Zintl phases which exhibit "locally delocalized electrons" mark the transition to the intermetallic phases.[5] The recent discovery of the transition-metal compounds $A_{14}MnPn_{11}$ (A = Ca, Sr, Ba; Pn = As, Sb, Bi), which are isostructural to main group Zintl compounds, provides a unique opportunity to study structure–property relationships at the border of Zintl and intermetallic compounds.

The synthesis, structure and properties of $A_{14}MnBi_{11}$ (A = Ca, Sr, Ba) compounds have been reported.[6] These compounds are isostructural with the known Zintl compounds, $A_{14}AlSb_{11}$ (A = Ca, Sr, Ba)[7,8] and $A_{14}GaAs_{11}$ (A = Ca, Sr).[9,10] If the Zintl concept is used to describe the bonding within the $A_{14}MPn_{11}$ (A = Ca, Sr, Ba; M = Al, Ga, Mn; Pn = As, Sb, Bi) structure type, then it can be described as containing 14 A^{2+} cations, a MPn_4^{9-} tetrahedron, a Pn_3^{7-} polyatomic anion, and 3 Pn^{3-} anions. This formal charge counting of the covalently bonded units implies that the valence of the metal is 3. It was expected that the magnetic properties for $A_{14}MnPn_{11}$ would be consistent with Mn^{III} and provide a moment indicative of a d^4 transition metal. Within the structure the Mn are situated about 10 Å apart, so it was surprising when temperature-dependent magnetic measurements indicated that $Ca_{14}MnBi_{11}$ and $Sr_{14}MnBi_{11}$ are ferromagnets with Curie temperatures (T_C) of 55 and 33 K, respectively. $Ba_{14}MnBi_{11}$ is an antiferromagnet with a Neel temperature (T_N) of 15 K. The high-temperature magnetic data are consistent with the Mn^{III} assignment. These three compounds have metallic resistivity and the magnetic exchange coupling can be attributed to a Ruderman–Kittel–Kasuya–Yosida (RKKY) interaction[11] between the localized moments via conduction electrons.

To study the properties and structural relationships of this structure type, we have prepared the antimony and arsenic analogs. As one prepares the lighter pnictide analogs, one would expect that the properties should change to semiconducting, resulting in loss of long-range magnetic order. Since there are main-group analogs of these compounds, in contrast to the Bi compounds, we can also compare their structure.

[†] Department of Chemistry.
[‡] Department of Physics.
[⊗] Abstract published in *Advance ACS Abstracts*, December 1, 1993.

(1) Nesper, R. *Prog. Solid State Chem.* **1990**, *20*, 1.
(2) Zintl, E. *Angew. Chem.* **1939**, *52*, 1.
(3) Eisenmann, B.; Schäfer, H. *Rev. Inorg. Chem.* **1981**, *3*, 29.
(4) Schäfer, H. *Annu. Rev. Mater. Sci.* **1985**, *15*, 1.
(5) Nesper, R. *Angew. Chem., Int. Ed. Engl.* **1991**, *30*, 789.
(6) Kuromoto, T. Y.; Kauzlarich, S. M.; Webb, D. J. *Chem. Mater.* **1992**, *4*, 435.
(7) Cordier, G.; Schäfer, H.; Stelter, M. *Z. Anorg. Allg. Chem.* **1984**, *519*, 183.
(8) Brock, S. L.; Weston, L. J.; Olmstead, M. M.; Kauzlarich, S. M. *J. Solid State Chem.*, in press.
(9) Kauzlarich, S. M.; Kuromoto, T. Y. *Croat. Chim. Acta* **1991**, *64*, 343.
(10) Kauzlarich, S. M.; Thomas, M. M.; Odink, D. A.; Olmstead, M. M. *J. Am. Chem. Soc.* **1991**, *113*, 7205.
(11) Kittel, C. *Solid State Phys.* **1968**, *22*, 1.

0897-4756/94/2806-0093$04.50/0

Table 1. Lattice Parameters from Room-Temperature Guinier X-ray Powder Diffraction Data

compound	a (Å)	c (Å)
$Ca_{14}MnSb_{11}$	16.742 (2)	22.314 (4)
$Sr_{14}MnSb_{11}$	17.530 (3)	23.354 (7)
$Ba_{14}MnSb_{11}$	18.395 (2)	24.266 (8)
$Ca_{14}MnAs_{11}$	15.785 (2)	21.041 (5)
$Sr_{14}MnAs_{11}$	16.575 (1)	22.229 (3)
$Ba_{14}MnAs_{11}$	17.433 (4)	23.264 (7)

Experimental Section

Materials. Crystalline dendritic calcium (99.99%), strontium (99.95%), and barium (99.9%) were obtained from Anderson Physics Labs. Manganese pieces (99.98%), polycrystalline arsenic lumps (99.99%), and antimony shot (99.9999%) were obtained from Johnson Matthey. The manganese pieces were first cleaned in a 5% HNO_3/MeOH solution and immediately transferred into a drybox.

Synthesis. The manganese flakes and pnictogen were ground into powders, and the alkaline earth metal elements were cut into small pieces in a drybox. All compounds were prepared by enclosing stoichiometric amounts of the elements in welded niobium tubes which were first cleaned with an acid solution (20% HF, 25% HNO_3, and 55% H_2SO_4). The sealed niobium tube was then sealed in a fused silica tube under low pressure ($\sim 1/5$ atm) of purified Ar. High yields (>95%) of either polycrystalline pieces or polycrystalline powders were obtained by heating the mixtures to temperatures between 950 and 1250 °C for periods between 24 h and 5 days and cooling the reaction to room temperature. The higher temperatures produced black needle crystals of $Sr_{14}MnSb_{11}$, black polygon crystals of $Ca_{14}MnSb_{11}$, $Ba_{14}MnSb_{11}$ and $Ba_{14}MnAs_{11}$, and black plates of $Ca_{14}MnAs_{11}$ and $Sr_{14}MnAs_{11}$. All reactions were opened, and their products examined in a nitrogen-filled drybox equipped with a microscope with typical water level less than 1 ppm. All the compounds are air sensitive, but the Ba compounds appear to be the most air sensitive and would "tarnish" in the drybox within several hours and decompose in the drybox within several days. We were unable to obtain either single-crystal X-ray diffraction data or reliable magnetic data on the $Ba_{14}MnAs_{11}$ because of the extreme air sensitivity of the sample.

Crystallography. X-ray powder diffraction patterns (room temperature, Cu $K\alpha_1$ radiation, wavelength = 1.540 562 Å) were obtained with an Enraf-Nonius Guinier powder camera. Sample mounting has been described previously.[6] Five silicon lines were fit by standard least-squares methods to known 2θ values and used to calculate the 2θ values for the sample lines. The powder patterns were indexed with the *hkl* values determined from calculated powder patterns.[12] The positions and intensities of the experimental diffraction lines agreed very well with the calculated diffraction pattern based on the single-crystal X-ray structures. The corresponding room-temperature lattice constants were determined by standard least-squares refinement and are given in Table 1.

Single-crystal X-ray data were obtained for all compounds except $Ba_{14}MnAs_{11}$, which appear to be more air-sensitive than the other compounds. The air-sensitive crystals were coated with paratone N oil in the drybox to protect them from air. A suitable crystal was mounted on a glass fiber with silicone grease and positioned in a cold stream of nitrogen. The single-crystal diffraction data for $Ca_{14}MnSb_{11}$ (0.0375 × 0.05 × 0.1 mm) and $Ba_{14}MnSb_{11}$ (0.125 × 0.1 × 0.05 mm) were collected at 130 K on a Syntex $P2_1$ diffractometer equipped with a modified Lt-1 low-temperature apparatus. The data for $Sr_{14}MnSb_{11}$ (0.25 × 0.05 × 0.02 mm), $Ca_{14}MnAs_{11}$ (0.5 × 0.01 × 0.005 mm), and $Sr_{14}MnAs_{11}$ (0.2 × 0.08 × 0.06 mm) were collected at 130 K on a Siemens R3m diffractometer. Rotation and axial photos were used to determine if the crystal was suitable for data collection. Unit cell parameters were obtained from least-squares refinement of about 10–24 reflections with $10° < 2\theta < 35°$. No decomposition of the crystals were observed (inferred from the intensity of two or three check reflections). The *I* centering was verified for the structures from systematic extinctions, and the cell dimensions were confirmed from axial photographs. There is no evidence for a super lattice or alternate space group for these compounds. Crystallographic parameters are summarized in Table 2. The data were corrected for Lorentz and polarization effects. Crystallographic programs used were those of SHELXTL PLUS Version 4.0.[13] in all cases except in the case of $Ca_{14}MnAs_{11}$. $Ca_{14}MnAs_{11}$ was refined using SHELX92.[14] Scattering factors and corrections for anomalous dispersion were taken from the *International Tables*.[15]

The initial atomic positions for all the compounds were taken from $Ca_{14}AlSb_{11}$[7] and refined by least-squares methods. In the case of $Sr_{14}MnAs_{11}$ and $Ba_{14}MnSb_{11}$, it was noted that the *U*'s (U_{11}, U_{22}) for the central Pn (Pn(4)) in the linear chain were large along the direction of the chain. This has also been observed in the $A_{14}GaAs_{11}$ (A = Ca, Sr)[9,10] and $A_{14}AlSb_{11}$ (A = Ca, Sr, Ba) compounds[8] and is attributed to positional disorder of the central Pn. A disorder model similar to that used for $Sr_{14}GaAs_{11}$,[9] where the site is half occupied, was used in the final stages of refinement to account for the disorder of the Pn(4) position. This model positions two Pn atoms unreasonably close together (0.80 (1) Å in $Sr_{14}MnAs_{11}$ and 0.581 (14) Å in $Ba_{14}MnSb_{11}$), but it adequately accounts for the positional disorder of the Pn(4) position. The data were corrected for absorption,[16,17] and refined with anisotropic *U*'s (except As(4) in $Sr_{14}MnAs_{11}$ and Sb(4) in $Ba_{14}MnSb_{11}$) to convergence.

The largest feature in the final difference map for $Ba_{14}MnSb_{11}$ is 7 $e^-/Å^3$ and is found 0.9 Å from Sb(3), the remaining features are less than 2 $e^-/Å^3$. The largest feature in the final difference maps for $Ca_{14}MnSb_{11}$, $Sr_{14}MnSb_{11}$, $Ca_{14}MnAs_{11}$, and $Sr_{14}MnAs_{11}$ is about 2 $e^-/Å^3$. Atomic coordinates, isotropic thermal parameters, anisotropic thermal parameters, and the observed and calculated structure factor amplitudes for each structural solution are given as supplemental material (see paragraph at end of paper).

Magnetic Susceptibility. Magnetic susceptibility measurements were made on a Quantum Design SQUID magnetometer at temperatures between 5 and 300 K. The samples were either polycrystalline powders or small chunks sealed in fused silica tubes under vacuum. The samples were cooled either in zero field or in a field of 1000–5000 G for measurements of magnetization versus temperature. Measurements were collected every 5 K around the ordering temperatures and then every 10 K at higher temperatures. Magnetization versus magnetic field measurements at either 6 or 10 K were obtained at fields between 0 and 10 000 G. For all compounds, data have been obtained on more than one sample to ensure reproducibility. Reliable magnetic data could not be obtained for the $Ba_{14}MnAs_{11}$. Due to the extreme air sensitivity of the compound, only one sample was run which exhibited Curie–Weiss behavior but gave a μ_{eff} = 7.2 μ_B.

Resistivity. Electrical resistivity measurements were made on sintered (950 °C for 3 days) pressed pellets (7000 psi) for $A_{14}MnAs_{11}$ (A = Ca, Sr, Ba). Resistivity measurements for $A_{14}MnSb_{11}$ (A = Ca, Sr, Ba) were made on polycrystalline pieces obtained from the melt. An in-line four-probe method was used for measuring all compounds. A constant current ranging from 5 μA to 5 mA was applied to the sample through the two outer leads (Keithley Model 224 current source), and the voltage was measured across the inner two leads (Keithley Model 196 microvoltmeter). Samples were mounted in the drybox onto a homemade sample holder to protect them from air and moisture. Indium was placed on the tips of four spring steel leads which were clamped onto the sample. Once enclosed in this holder, the

(12) Clark, C. M.; Smith, D. K.; Johnson, G. J. *POWDER5*, A FORTRAN IV Program for calculating X-ray diffraction Patterns, 5, Department of Geosciences, Pennsylvania State University, University Park, PA, 1973.

(13) Sheldrick, G. M., *SHELXTL PLUS, A Program for Crystal Structure Determination*, 4.0, 1989, Madison, WI.

(14) Sheldrick, G. *J. Appl. Crystallogr.*, in press.

(15) *International Tables for Crystallography*; Reidel Publishing Co.: Boston, 1992; Vol. C.

(16) Hope, H.; Moezzi, B.; *XABS*, Program XABS provides an empirical correction based on F_o and F_c differences, Chemistry Department, University of California, Davis.

(17) Parkin, S.; Hope, H.; Moezzi, B., *XABS2*, Program XABS2 provides an empirical correction based on F_o^2 and F_c^2 differences, Department of Chemistry, University of California, Davis.

Table 2. Crystallographic Parameters for Compounds of the Formula $A_{14}MnPn_{11}$ (A = Ca, Sr, Ba; Pn = As, Sb) ($I4_1/acd$, $Z = 8$)

formula	$Ca_{14}MnAs_{11}$	$Sr_{14}MnAs_{11}$	$Ca_{14}MnSb_{11}$	$Sr_{14}MnSb_{11}$	$Ba_{14}MnSb_{11}$
a, Å	15.714 (3)	16.576 (10)	16.688 (8)	17.511 (4)	18.394 (3)
c, Å	21.141 (6)	22.167 (14)	22.266 (9)	23.321 (7)	24.069 (6)
V, Å^3	5220 (2)	6091 (15)	6201 (5)	7151 (4)	8144 (6)
μ (Mo Kα), cm^{-1}	171	365	121	292	207
transm coeff range	0.04–0.40	0.10–0.22	0.54–0.68	0.02–0.24	0.11–0.16
$2\theta_{max}$	55	55	55	50	60
no. obsd refns	1060 [$F > 4\sigma(F)$]	941 [$F > 4\sigma(F)$]	1143 [$F > 6\sigma(F)$]	1058 [$F > 4\sigma(F)$]	1232 [$F > 4\sigma(F)$]
no. params refined	60	60	61	61	60
R^a	4.09	5.70	5.82	4.07	7.52
$R_w{}^a$ [$w = 1/\sigma^2(F_o)$]	8.82[b]	4.87	6.95	3.93	6.96

[a] $R = \Sigma||F_o| - |F_c||/|F_c|$ and $R_w = \Sigma||F_o| - |F_c||w^{1/2}/\Sigma|F_o w^{1/2}|$. [b] $wR2 = [\Sigma[w(F_o^2 - F_c^2)^2]/\Sigma[(wF_o^2)^2]]^{1/2}$.

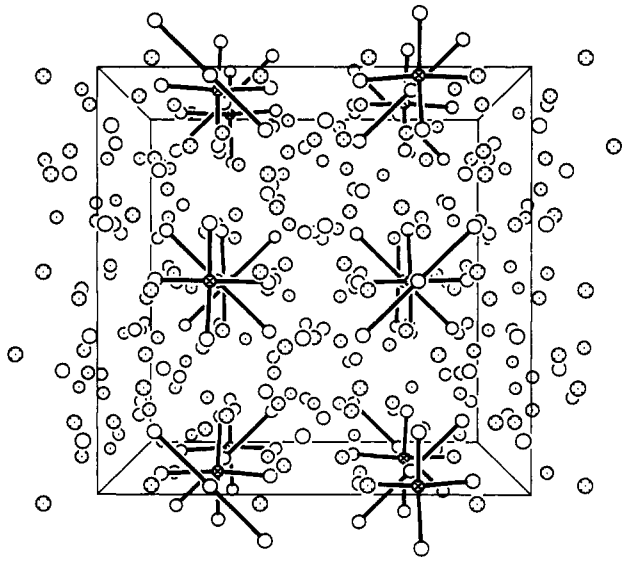

Figure 1. Perspective view along the c axis of the unit cell of $A_{14}MnPn_{11}$ (A = Ca, Sr, Ba; Pn = As, Sb). The crossed, open, and dotted circles represent Mn, Pn, and A, respectively.

sample could be transferred to the closed-cycle He refrigerator without exposure to air. The sample was cooled to approximately 10 K, and its resistivity measured in 1 K increments around the magnetic ordering temperatures and then every 5 K up to 300 K.[18]

Results and Discussion

Structure. The transition-metal ternary compounds $A_{14}MnPn_{11}$ (A = Ca, Sr, Ba; Pn = As, Sb) are isostructural with the main-group Zintl compounds $A_{14}AlSb_{11}$ (A = Ca, Sr, Ba)[7,8] and $A_{14}GaAs_{11}$ (A = Ca, Sr).[9,10] The $A_{14}MPn_{11}$ (M = Al, Ga, Mn) structure type has been described in the framework of the Zintl–Klemm concept. The formal charges for one formula unit of the $A_{14}MPn_{11}$ materials are assigned as follows: $14A^{2+}$, $4Pn^{3-}$, $MnPn_4{}^{9-}$, and $Pn_3{}^{7-}$. The structure type has been described in detail previously.[6,7,19,20] Figure 1 shows a perspective view of the unit cell. Briefly, the $MnPn_4$ tetrahedra and the Pn_3 linear chains alternate with respect to one another along the c axis. The chains are rotated by 90° with respect to one another along the c axis. The chains and tetrahedra alternate with each other along the a and b axes as well but are translated by a full unit cell dimension along these directions. Selected bond distances and angles for $A_{14}MnPn_{11}$ (A = Ca, Sr, Ba and Pn = As, Sb) can be found in Table 3.

Figure 2 shows the $MnPn_4$ tetrahedron and the polyatomic linear anion with selected cations. The $MnPn_4$ tetrahedra are slightly distorted and are flattened along the a–b plane. The angles in the tetrahedra of the Sb and As analogs do not change in a smooth fashion with the size of cation ($(Ca_{14}MnSb_{11})$ 106.6° and 115.3°, $(Sr_{14}MnSb_{11})$ 106.4° and 115.9°, $(Ba_{14}MnSb_{11})$ 105.1° and 118.7°, $(Ca_{14}MnAs_{11})$ 107.1° and 114.4°, and $(Sr_{14}MnAs_{11})$ 106.9° and 114.7°), in contrast to the Bi analogs, where the distortion increases by almost 1° as a function of increasing cation size. The main-group analogs also have distorted tetrahedra, for example, in $Ca_{14}AlSb_{11}$, the angles are 114.0° and 107.3°, slightly smaller than the transition-metal compound. The larger distortion observed in the Mn compounds compared with the main group analogs is attributed to a Jahn–Teller effect (Mn^{III} is a d^4 ion),[19] although steric effects probably also contribute.[8]

As expected for increasing anion size, the Mn–Pn distances increase as the pnictogen is changed from As to Sb to Bi (2.599 (1) Å for $Ca_{14}MnAs_{11}$, 2.759 (2) Å for $Ca_{14}MnSb_{11}$, and 2.889 (1) Å for $Ca_{14}MnBi_{11}$). Typical Mn–Pn bond lengths range from 2.57 to 2.77 Å for Pn = As,[21–23] 2.74 to 2.83 for Pn = Sb,[22,24–26] and 2.82 to 2.96 Å in Pn = Bi compounds.[25,27,28]

The Sb–Sb distances in the linear chain increase as a function of increasing electron donor ability from 3.215 (1) Å (Ca) to 3.310 (1) Å (Sr). These distances are comparable with those observed in the main-group analogs, $A_{14}AlSb_{11}$ (3.196 (2) Å–3.370 (2) Å). The distances are larger than a Sb–Sb single bond (2.84–2.91 Å),[29] but the increased distance is consistent with the interpretation of a 2-center 4-electron bond.[30] In the case of $Ba_{14}MnSb_{11}$, a disordered model most accurately fits the single-crystal X-ray data where the $Sb_3{}^{7-}$ unit has two inequivalent

(18) Sunstrom, J. E., IV, *DCRES: A quickbasic program for temperature dependent resistivity data collection and analysis*, 1991, University of California, Davis.
(19) Kauzlarich, S. M.; Kuromoto, T. Y.; Olmstead, M. M. *J. Am. Chem. Soc.* **1989**, *111*, 8041.
(20) Kauzlarich, S. M. *Comments Inorg. Chem.* **1990**, *10*, 75.
(21) Mewis, A. *Z. Naturforsch.* **1978**, *33b*, 606.
(22) Brechtel, E.; Cordier, G.; Schäfer, H. *Z. Naturforsch* **1979**, *34b*, 777.
(23) Dietrich, L. H.; Jeitschko, W.; Möller, M. H. *Z. Kristallogr.* **1990**, *190*, 259.
(24) Brechtel, E.; Cordier, G.; Schäfer, H. *Z. Naturforsch.* **1979**, *34b*, 921.
(25) Cordier, G.; Schäfer, H. *Z. Naturforsch.* **1976**, *31b*, 1459.
(26) Reimers, W.; Hellner, E.; Treuttianan, W.; Brown, P. J. *J. Phys. Chem. Solids* **1983**, *44*, 195.
(27) Brechtel, E.; Cordier, G.; Schäfer, H. *Z. Naturforsch.* **1980**, *35b*, 1.
(28) Brechtel, E.; Cordier, G.; Schäfer, H. *Z. Naturforsch.* **1979**, *34b*, 1229.
(29) Wells, A. F. *Structural Inorganic Chemistry*, 5th ed.; Oxford University Press: Oxford, UK, 1984.
(30) Gallup, R. F.; Fong, C. Y.; Kauzlarich, S. M. *Inorg. Chem.* **1992**, *31*, 115.

Table 3. Selected Bond Lengths (Å) and Angles (deg)

		$Ca_{14}MnAs_{11}$	$Sr_{14}MnAs_{11}$		$Ca_{14}MnSb_{11}$	$Sr_{14}MnSb_{11}$		$Ba_{14}MnSb_{11}$
Pn(1)–Pn(4)	×2	2.730 (2)	2.750 (6)	×4	3.215 (2)	3.310 (2)	×2	3.127 (8)
	×2	3.308 (6)	3.448 (8)				×2	3.709 (8)
Pn(1)–A(1) ×2		3.033 (2)	3.192 (3)		3.220 (4)	3.368 (2)		3.510 (3)
Pn(1)–A(2) ×2		3.059 (2)	3.232 (3)		3.280 (4)	3.441 (2)		3.647 (3)
Pn(1)–A(3) ×2		3.199 (2)	3.377 (3)		3.373 (2)	3.561 (2)		3.723 (2)
Pn(1)–A(4) ×2		3.036 (2)	3.222 (4)		3.192 (4)	3.376 (2)		3.589 (4)
Pn(2)–Mn(1) ×4		2.603 (1)	2.683 (3)		2.759 (2)	2.838 (1)		2.872 (3)
Pn(2)–A(1)		3.015 (2)	3.211 (4)		3.189 (4)	3.366 (2)		3.571 (4)
Pn(2)–A(1′)		3.024 (2)	3.217 (3)		3.204 (4)	3.388 (2)		3.610 (3)
Pn(2)–A(2)		3.562 (2)	3.712 (4)		3.750 (4)	3.873 (2)		4.003 (4)
Pn(2)–A(2′)		2.938 (2)	3.086 (3)		3.137 (4)	3.273 (2)		3.423 (4)
Pn(2)–A(3)		3.092 (2)	3.305 (3)		3.258 (4)	3.452 (2)		3.679 (3)
Pn(2)–A(4)		2.970 (2)	3.115 (4)		3.172 (4)	3.306 (2)		3.468 (4)
Pn(2)–A(4′)		3.178 (2)	3.310 (4)		3.403 (4)	3.526 (2)		3.672 (4)
Pn(3)–A(1)		3.071 (2)	3.235 (4)		3.240 (4)	3.392 (2)		3.536 (4)
Pn(3)–A(1′)		3.021 (2)	3.190 (4)		3.206 (4)	3.362 (2)		3.518 (4)
Pn(3)–A(2)		3.090 (2)	3.251 (4)		3.314 (4)	3.481 (2)		3.634 (4)
Pn(3)–A(2′)		2.980 (2)	3.159 (4)		3.175 (4)	3.371 (2)		3.537 (4)
Pn(3)–A(3)		2.948 (2)	3.095 (4)		3.140 (4)	3.304 (2)		3.449 (4)
Pn(3)–A(4)		3.069 (2)	3.251 (4)		3.252 (4)	3.409 (2)		3.519 (4)
Pn(3)–A(4′)		3.097 (2)	3.254 (4)		3.249 (4)	3.426 (2)		3.531 (4)
Pn(3)–A(4″)		3.632 (2)	3.846 (4)		3.775 (4)	4.004 (2)		4.132 (4)
Pn(4)–A(1)	×2	2.895 (2)	3.024 (3)	×4	3.210 (4)	3.384 (2)	×2	3.423 (4)
	×2	3.181 (2)	3.416 (4)				×2	3.709 (5)
Pn(4)–A(2)	×2	3.082 (2)	3.215 (4)	×4	3.410 (4)	3.584 (2)	×2	3.675 (4)
	×2	3.383 (2)	3.624 (4)				×2	3.962 (5)
Mn–A(2) ×4		3.439 (2)	3.577 (3)		3.591 (4)	3.721 (2)		3.795 (3)
Mn···Mn		9.471 (2)	9.970 (3)		10.030 (4)	10.519 (3)		10.991 (5)
Pn(2)–Mn–Pn(2′)		107.5 (1)	106.9 (1)		106.6 (1)	106.4 (1)		105.1 (1)
Pn(2)–Mn–Pn(2″)		113.4 (1)	114.7 (1)		115.3 (1)	115.9 (1)		118.7 (1)

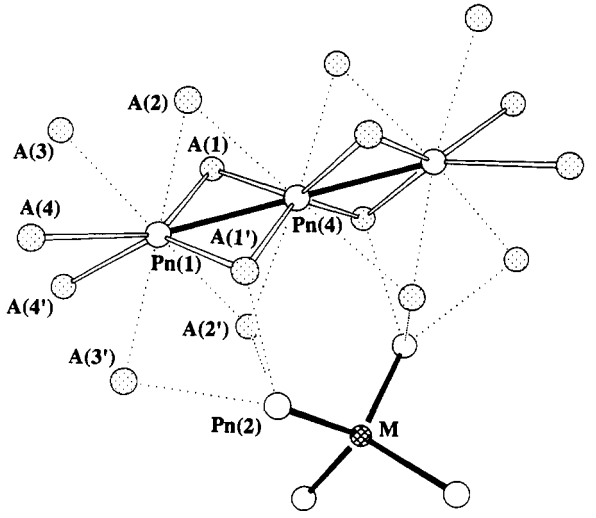

Figure 2. View of the polyatomic units Pn_3^{7-} and $MnPn_4^{9-}$, with selected cations, showing their relative orientation with respect to each other.

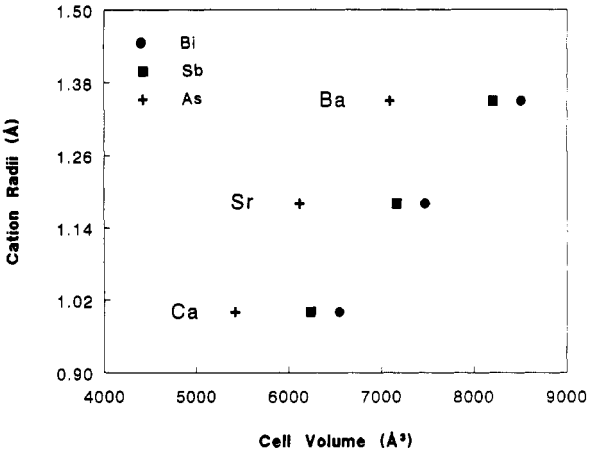

Figure 3. Cation ionic radii versus the volumes of the compounds, $A_{14}MnPn_{11}$ (A = Ca, Sr, Ba, and Pn = As, Sb, Bi).

distances of 3.127 and 3.709 Å. The As–As bond is long (3.013 Å) in the As_3^{7-} unit in $Ca_{14}MnAs_{11}$ and slightly larger than what is observed for $Ca_{14}GaAs_{11}$ (2.956 Å). Similar to $Ba_{14}MnSb_{11}$, the As–As distance in the As_3^{7-} unit of $Sr_{14}MnAs_{11}$ is apparently too long to give a symmetrically bonded arrangement of the As_3^{7-} unit. The As_3^{7-} unit is asymmetric with one long and one short bond, 3.448 (8) and 2.750 (6) Å (Sr), similar to what is observed in $Sr_{14}GaAs_{11}$.[9] Typical As–As single-bond distances are about 2.4–2.5 Å.[31,32]

Figure 3 shows the cation ionic radii[33] versus the volumes of the compounds, $A_{14}MnPn_{11}$ (A = Ca, Sr, Ba, and Pn = As, Sb, Bi). Just as there is the semiconductor–metal division between As and Sb, there is a break in the volumes of each cation series between As and Sb. One might expect, based on this figure, that the properties of the Bi and Sb analogs should be similar.

Magnetic and Electrical Properties. Figures 4 and 5 show inverse magnetic susceptibility versus temperature data for the Sb and As analogs, respectively. The Curie constants, the paramagnetic Curie temperatures (Weiss constants) θ, and the background susceptibilities determined from fits to these data are given in Table 4.

The susceptibility for each of the compounds is consistent with a local moment due to four unpaired spins on each Mn ion, confirming the assignment of +3 for the Mn valence. The paramagnetic Curie temperatures suggest that all the Sb compounds have magnetically coupled Mn spins with coupling strengths of the same order of magnitude as the Bi analogs. Changing the cation in these materials has a much larger effect on the coupling than

(31) Deller, K.; Eisenmann, B. *Z. Naturforsch.* **1977**, *32b*, 1368.
(32) Verdier, P.; L'Haridon, P.; Mauaye, M.; Laurent, Y. *Acta Crystallogr.* **1976**, *B32*, 726.
(33) Shannon, R. D. *Acta Crystallogr.* **1976**, *A32*, 751.

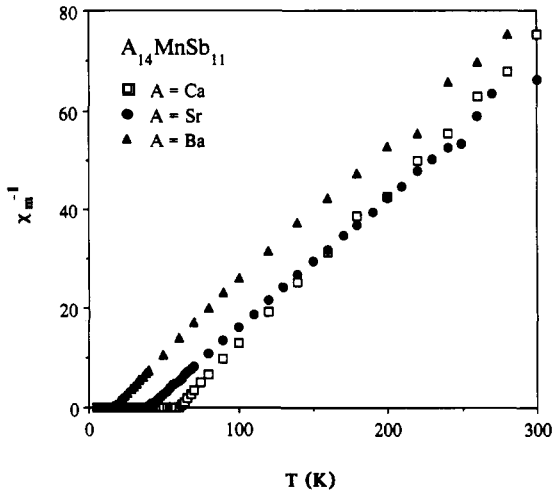

Figure 4. Inverse magnetic susceptibility versus temperature for $A_{14}MnSb_{11}$ (A = Ca, Sr, Ba).

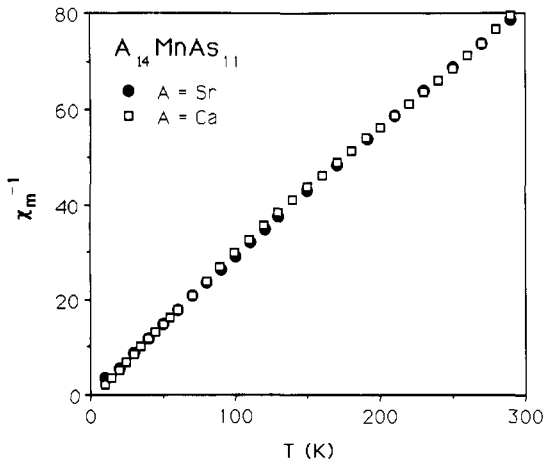

Figure 5. Inverse magnetic susceptibility versus temperature for $A_{14}MnAs_{11}$ (A = Ca, Sr, Ba).

changing from Sb to Bi. The As analogs have Mn moments which are relatively uncoupled from each other.

Figure 6 shows the magnetization in a field of 100 Oe at low temperature for the Sb compounds. The three compounds are all apparently ferromagnetic: the paramagnetic Curie temperature, θ, is positive; the magnetization measured at $H = 100$ Oe rises sharply below a well-defined temperature, T_C, which is approximately equal to θ; and the low-temperature magnetization versus field data show a characteristic ferromagnetic shape. Figure 7 shows the low-temperature magnetization versus field data for each Sb compound. As mentioned above, it is surprising, considering that the nearest Mn–Mn distance (six Mn near neighbors) is about 10 Å, that the Mn spins are magnetically coupled. Mn spins 10 Å apart are unlikely to be coupled together by direct overlap of wave functions. Therefore, if the Mn spins can be regarded as localized, then the exchange interaction between the Mn spins must be via some intervening electron states, either localized orbitals (superexchange)[34] or extended states (RKKY-type exchange observed in metals or semiconductors[35]). Electronic structure calculations on an isostructural compound, $Ca_{14}GaAs_{11}$, suggest that superexchange between Mn through several intervening ions is unlikely to be important.[30] If the Zintl concept is valid, then the metallic conductively observed in the Bi analogs is due to overlap of the conduction band with the valence band. One might expect, based on this interpretation, that the Sb analogs will be similar to Bi and behave as metals, whereas the As analogies will be semiconductors and will not magnetically order. If this is true, we can conclude that the Mn–Mn exchange is primarily through an RKKY-type interaction.

The Mn–Mn coupling increases as either the cation or the anion is made smaller. Figure 8 shows θ as a function of the Mn–Mn distance for all of the $A_{14}MnSb_{11}$ and $A_{14}MnBi_{11}$ compounds. Figure 8 clearly shows that the Mn–Mn coupling strength increases smoothly as a function of decreasing Mn–Mn distance. We take the well-behaved nature of this increase as an indication that all of the Sb and Bi compounds have similar electronic structure. We expect that these compounds are very similar electronically and that the transition temperature is largely determined by the Mn–Mn distances.

We can take the above conclusions further by comparing the data with predictions of the RKKY theory of magnetic coupling. We do not know much about the conduction electrons in these materials so we will use the simple free electron isotropic RKKY theory to parameterize the data. We use as an estimate of the paramagnetic Curie temperature $\theta = NS(S+1)A(2k_F)^3F(r)$, where N is the number of Mn neighbors, $S = 2$ is the Mn local spin, A is an overall scale factor which depends both on the polarizability of the conduction electrons and on the exchange interaction between conduction electrons and the Mn spins, k_F is the Fermi wavevector, $F(r) = [2k_Fr\cos(2k_Fr) - \sin(2k_Fr)]/(2k_Fr)^4$ is the function giving the distance dependence of the magnetic interaction, and r is the Mn–Mn distance. We use $N = 10$ because there are 10 Mn nearest neighbors at distances between 10 and 11 Å. The next order correction would be to include the six second-nearest neighbors which probably also have strong interactions. This is reflected in the fact that $Ba_{14}MnBi_{11}$ orders antiferromagnetically even though $\theta > 0$ for this compound.[36] The solid line in Figure 8 represents this parametrization of the data on the Sb and Bi compounds with $k_F = 0.5$ Å^{-1} and $A = 1 \times 10^{-37}$ erg cm^3. It is probably best in this analysis to consider k_F as a parameter which sets the length scale of the interaction and A as a parameter related to the strength of the interaction between a conduction electron and a local Mn spin.

If we interpret the length scale parameter, k_F, as the Fermi wavevector, the fit implies a low electron density (3×10^{21} cm^{-3}) metal which is not surprising considering the structure of the compound. Analysis of the structure suggests that the bonding between the anions and cations is primarily ionic, and therefore any metallic state is essentially incidental. In any case, whether these materials are semimetals or nearly zero-gap semiconductors, one expects the length scale for exchange interactions determined by an RKKY-type theory to be large. This is consistent with the strong coupling seen at distances as large as 10 Å. The value of A from comparison with the RKKY theory is about the same magnitude as that for Mn dissolved in Au[37] and so suggests a reasonable coupling strength between the Mn local spins and conduction and/

(34) In *Magnetism*; Rado, G. T., Suhl, H., Eds.; Academic Press: New York, 1963.
(35) (a) Liu, L. *Solid State Commun.* **1980**, *35*, 187. (b) Liu, L. *Phys. Rev. B* **1982**, *26*, 6300.
(36) Webb, D. J.; Kuromoto, T. Y.; Kauzlarich, S. M. *J. Magn. Magn. Mater.* **1991**, *98*, 71.
(37) Smith, F. W. *Phys. Rev. B* **1976**, *14*, 241.

Table 4. Resistivity and Magnetic Data for $A_{14}MnPn_{11}$ (A = Ca, Sr, Ba; Pn = As, Sb)

compound	ρ_{300K} (Ω cm)	E_a (eV)	T_C (K)	θ (K)	C	χ_0 (emu/mol)	μ_{eff} (μ_B)	μ_{sat} (μ_B)
$Ca_{14}MnAs_{11}$	10^{-1}	0.18(1)			3.3(1)	$1.4(7) \times 10^{-4}$	5.2(1)	
$Sr_{14}MnAs_{11}$	10^{1}	0.25(1)			3.5(1)	$3.4(1) \times 10^{-3}$	5.1(1)	
$Ba_{14}MnAs_{11}$	10^{3}	0.38(1)						
$Ca_{14}MnSb_{11}$	10^{-3}		65	62(1)	3.3(1)	$1.5(2) \times 10^{-3}$	5.2(1)	2.7(1)
$Sr_{14}MnSb_{11}$	10^{-3}		45	40(1)	3.6(1)	$4.2(8) \times 10^{-4}$	5.4(1)	3.3(1)
$Ba_{14}MnSb_{11}$	10^{0}		20	18(1)	3.0(1)	$6(1) \times 10^{-4}$	4.9(1)	2.2(1)

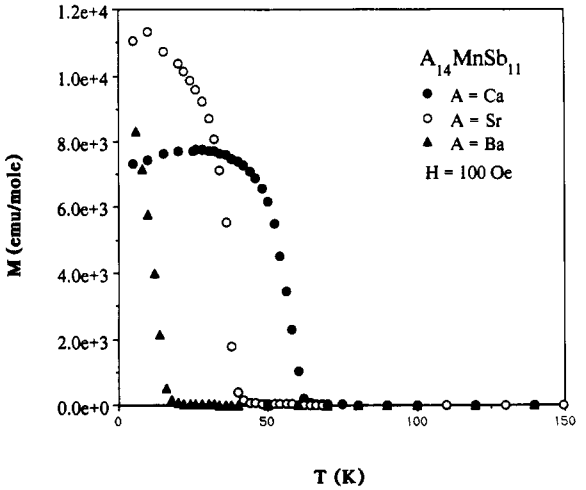

Figure 6. Magnetization in a field of 100 Oe at low temperature for $A_{14}MnSb_{11}$ (A = Ca, Sr, Ba).

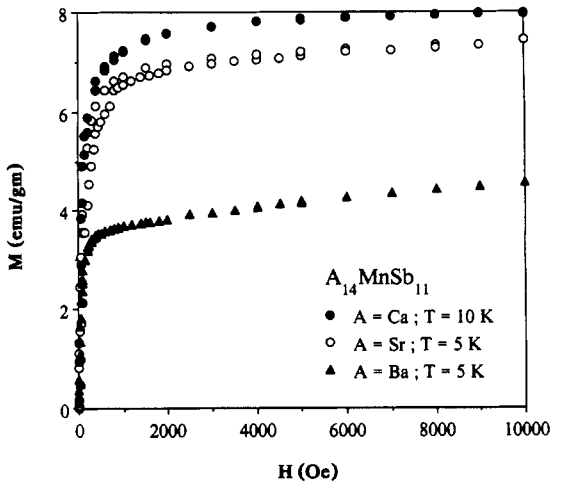

Figure 7. Low-temperature hysteresis loops for $A_{14}MnSb_{11}$ (A = Ca, Sr, Ba).

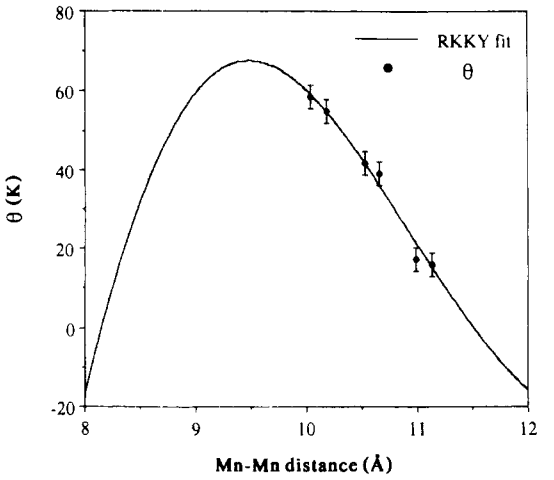

Figure 8. Weiss constant, θ, plotted as a function of the Mn···Mn distance for all of the $A_{14}MnSb_{11}$ and $A_{14}MnBi_{11}$ (A = Ca, Sr, Ba) compounds. The solid line represents the parametrization of the data to the simple free electron isotropic RKKY theory with $k_F = 0.5$ Å^{-1} and $A = 1.5 \times 10^{-37}$ erg em^3.

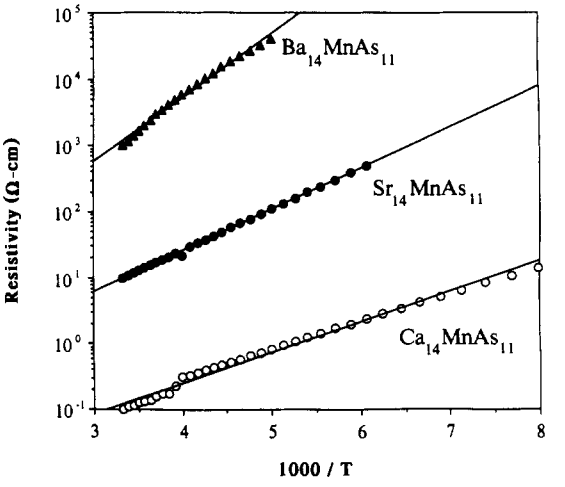

Figure 9. Resistivity versus $1000/T$ for $A_{14}MnAs_{11}$ (A = Ca, Sr, Ba).

or valence electrons. There are several reasons for suggesting that the coupling is not due to an accidental doping of these materials. First, single-crystal data and lattice parameters from powder data indicate that there is no compositional nonstoichiometry. There is also no variability in the T_c of these compounds from preparation to preparation and the Mn–Mn distance dependence of θ is smooth. In contrast, we should note that samples of $A_{14}MnAs_{11}$ (A = Ca, Sr, Ba) have magnetic states which are quite sensitive to the preparation conditions.[38] This is attributed to small and accidental doping or nonstoichiometry of these magnetic semiconductors. The most stoichiometric and high quality samples of $A_{14}MnAs_{11}$ have perfect Curie behavior.

The temperature dependence of the resistivity of the As compounds is shown in Figure 9 as resistivity versus $1000/T$. These compounds are apparently semiconducting and confirm the conclusions surmised from an examination of the magnetic data. The activation energies derived from Figure 9 are listed in Table 4. The activation energies decrease as a function of decreasing cation size implying that $Ca_{14}MnAs_{11}$ is a narrow-gap semiconductor.

Figure 10 shows the temperature dependence of the resistivity of the Sb compounds. The temperature dependence of the resistivities of the Sb compounds is more difficult to understand. At first sight, the increase in resistivity as a function of decreasing temperature suggests that these materials may also be semiconductors. However, there is a drop in resistivity below the magnetic ordering temperature. If the low-temperature drop in resistivity is as large as the high-temperature rise (and in some cases it is) then it is possible that the resistivity

(38) Del Castillo, J.; Webb, D. J.; Kauzlarich, S. M.; Kuromoto, T. Y. *Phys. Rev. B* **1993**, *47*, 4849.

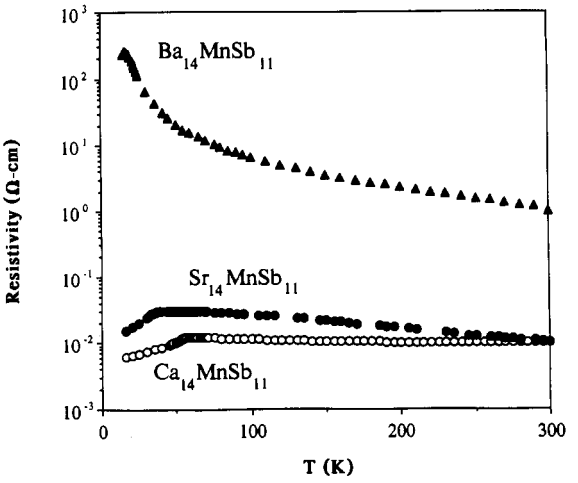

Figure 10. Resistivity versus temperature for $A_{14}MnSb_{11}$ (A = Ca, Sr, Ba).

increase as the temperature is lowered toward T_C is simply due to magnetic disorder which disappears below T_C. These data, both the temperature dependence and the magnitude of the resistivity changes, are reminiscent of some of the heavy Fermion compounds[39] where the resistivity maximum presumably also signals a decrease in the scattering due to magnetic disorder. However, in the case of the heavy Fermion compounds, there is no evidence that the magnetic disorder disappears at the temperature of the peak. Instead, it is suspected that the magnetic disorder becomes less effective in the scattering due to the formation of a new conduction electron state in which the scattering from magnetic electrons is coherent and the resistivity is lower. For the $A_{14}MnSb_{11}$ compounds, it is clear that the magnetic disorder decreases below the magnetic transition and that this causes the maximum.

In the simplest case, these compounds are Zintl compounds where the valence band is full and the conduction band is empty. The magnetic coupling is attributed to a RKKY-type interaction. As the anion is changed from Bi to Sb, the overlap between the valence and conduction band becomes smaller, and for the As compounds, there is no overlap between the valence and conduction band. In this manner, these materials are true Zintl compounds. Pressure measurements on $Sr_{14}MnAs_{11}$[38] support this rather simple hypothesis. Further research on single crystals is underway to help understand the electronic properties of these materials.

Acknowledgment. We thank M. M. Olmstead for assistance with the structure determinations and R. N. Shelton and P. Klavins for use of the magnetometer and assistance in resistivity measurements. A.R. was supported by a fellowship from the Deutsche Forschungsgemeinschaft. Financial support from the National Science Foundation, Division of Materials Research (DMR-9201041 (S.M.K.) and DMR-8913855 (D.J.W.)), is gratefully acknowledged.

Supplementary Material Available: Additional diffraction and refinement data, anisotropic displacement parameters for $A_{14}MnSb_{11}$ and $A_{14}MnAs_{11}$ (A = Ca, Sr, Ba) (4 pages); tables of observed and calculated structure factors (34 pages). Ordering information is given on any current masthead page.

(39) Fisk, Z.; Ott, H. R.; Rice, T. M.; Smith, J. L. *Nature* **1986**, *320*, 124.